ISBN: 978-3-95450-217-2 doi:10.18429/JACoW-ERL2019-WEPNEC21

Decoupling Cathode and Lattice Emittance Contributions from a 100 pC, 100 MeV Electron Injector System

N.P. Norvell*, SLAC National Accelerator Lab, Menlo Park and UC Santa Cruz, CA USA
M.B. Andorf, I.V. Bazarov, J.M. Maxson, C. Gulliford
Center for Bright Beams, Cornell University, Ithaca NY, USA

Abstract

We present simulation results to decouple the emittance contributions that are intrinsic from the injector lattice versus emittance contributions due to the quality of the cathode out of a 100 MeV electron injector system. Using ASTRA driven by the NSGA-II genetic algorithm, we optimized the LCLS-II injector system with a zero emittance cathode. We then imposed FEL specific energy constraints and show how the Pareto Front solution shifts. Lastly, we reoptimized at various cathode emittances to map out the dependence of cathode emittance versus final emittance out of the injector system. We then determined the cathode quality needed to hit a 0.1 mm mrad 95% rms transverse emittance specification out of the current LCLS-II injector system.

SIMULATION MOTIVATION

SLAC National Accelerator Lab is currently constructing a MHz repetition rate Free Electron Laser (FEL), the Linac Coherent Light Source II, to follow up the success of the 120 Hz LCLS. LCLS-II will initially run with a 4 GeV superconducting linac but plans are underway to upgrade the linac further to accelerate electrons to 8 GeV for LCLS-II HE (High Energy), increasing the maximum deliverable x-ray energy up to almost 15 keV[1]. Even after the upgrades to the LCLS-II facilities, FEL users would still like a higher photon range from the LCLS-II complex. At higher electron energies, the x-ray energy range becomes throttled by emittance if the number of undulator magnets are not increased[1]. Emittance directly determines how efficiently the electron beam microbunches, which is required to start the exponential growth of x-ray production in the undulators[2]. Currently, LCLS-II expects a transverse normalized emittance of 0.4 mm-mrad at the first undulator for a 100 pC electron beam. As shown in Fig. 1, simulations predict that decreasing the normalized emittance at the undulators from 0.4 to 0.1 mm-mrad with an 8 GeV electron beam would expand LCLS-II HE x-ray energy upper bound from 15 keV to 22 keV. The benefit from lower emittance is even more drastic for FELs driven with higher electron energies with a similar undulator hall.

The quality of the electron beams produced in an accelerator facility is inherently limited by the emittance of the beam produced in the injector system. We define the injector system as the beamline that takes the beam from a cathode to around 100 MeV, when space charge effects are

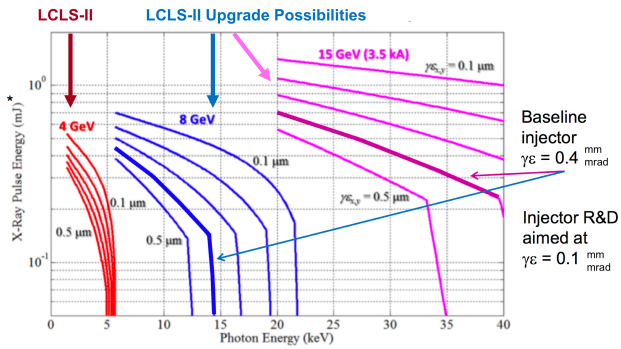

Figure 1: Expectations for how the emittance will effect the photon range for the LCLS-II and potential upgrades for various linac energies. The curves are predicted from the Ming Xie equations that numerically find the power gain length for x-ray generation[1].

no longer a concern. The current LCLS-II injector system simulations predict transverse emittances around 0.3 mm-mrad out of the injector, indicating that injector improvements are necessary and the correct place to start looking to improve the emittance [3]. In these proceedings, we investigate the emittance benefits for the LCLS-II injector we could expect from improving the cathode quality and determine how much we would have to improve the cathode by to deliver a beam with a 0.1 mm mrad 95% rms transverse emittance for the LCLS-II HE project.

OPTIMIZATION METHODOLOGY

We started with the optimization end point from the original LCLS-II optimization[4][5]. We used the particle tracking code ASTRA[6] driven by the multi-objective genetic algorithm NSGA-II [7] to compute and optimize two competing quantities, bunch length σ_z and the 95% rms horizontal emittance[8]. We get a set of solutions, called a Pareto Front, that visually documents the trade off between these two competing variables. We used a population size of 80 and ran all simulations with a bunch charge of 100 pC.

The first study documented the Pareto Front limit of an injector system. To isolate the lattice emittance contributions that are due to space charge, we turned off the cathode emittance by using ASTRA's generator program to create a radially uniform beam emerging from a zero longitudinal and transverse emittance source.

We imposed constraints to guide the optimizer to rea-

* nnorvell@slac.stanford.edu

ISBN: 978-3-95450-217-2 doi:10.18429/JACoW-ERL2019-WEPNEC21

Table 1: Parameters that were varied for the injector system. Zero degrees is defined as on crest for max acceleration and the field gradients are the value of the maximum field in the field file.

Knob	Variable Range
Transverse rms at cathode	0.05 - 2 mm
Bunch length at cathode	5 - 50 ps
Gun gradient	20.04 MV/m
Gun phase	-45 - 10 deg.
Solenoid 1 field	0.01- 0.2 T
Capture cavity gradient	0 - 2 MV/m
Capture cavity phase	-120 - 0 deg.
Solenoid field	0 - 0.2 T
Cavity 1 field	0 - 32 MV/m
Cavity 2 field	0 MV/m
Cavity 4 field	0 - 32 MV/m
Cavity 1 phase	-90 - 90 deg.
Cavity 4 phase	-90 - 90 deg.

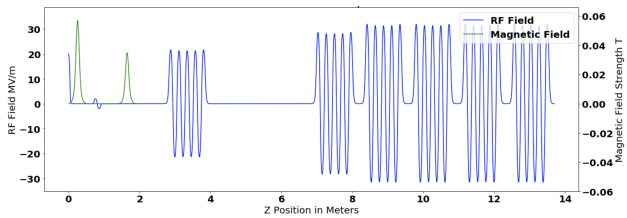

Figure 2: The field layout for the LCLS-II injector with the APEX gun.

sonable solutions. Constraints are binary conditions where configurations are initially ranked on the number of constraints violated. We required: a) The end energy is > 90 MeV, b) rms bunch length is less than 1.5 mm, c) 100% rms emittance is less than 1.0 mm mrad, d) Final energy spread < 500 keV, e) Higher Order (HO) Energy spread $<$ 50 keV, f) The average $x_{pos}x_{angle}$ is negative so we have a converging beam. HO energy spread is calculated by fitting a second order polynomial to the energy spread and finding an rms energy spread after subtracting out the polynomial of best fit.

We obtained a suitable front with a zero emittance cathode and then imposed more stringent energy constraints to determine how the Pareto Front would shift. First, we tightened the overall energy spread constraint from 500 keV to 200 keV. The 200 keV value matches previously performed LCLS-II optimization work and was imposed to ensure a sufficiently small energy spread at the undulator hall[5]. To save computing time, we seeded the NSGA-II algorithm with the final population from the zero emittance cathode run with looser energy constraints. We then continued optimizing for sufficient generations to get a satisfactory Pareto Front with the harder constraint.

We then took the end population with the tightened energy spread constraint and further tightened the higher order energy spread constraint from 50 keV to 5 keV.

We kept in the 200 keV energy spread and 5 keV HO energy spread constraints and started the next phase of the experiment to quantify how cathode emittance effects the Pareto Front. We set the cathode quality by specifying an emittance for the initial beam profile. We selected an isotropic momentum distribution, or radially uniform emission angles into a half sphere, to describe the beam off the cathode and realistically couple the initial transverse and longitudinal momentum spreads [9]. To help mitigate the legitimate problem of getting stuck in a local minimum, we started the cathode portion of the study with an unseeded, fresh run with a cathode having a thermal emittance (Temit) of 1 μm/ mm rms or a Mean Transverse Energy (MTE) of 510 meV. We filled in intermediary cathode emittances by seeding with population members from both the zero emittance cathode population with stricter energy constraints and the 1 μm/ mm rms cathode baseline.

CATHODE UPGRADE RESULTS

LCLS-II is using the 187 MHz gun developed for the Advanced Photoinjector Experiment (APEX)[10]. Past simulation results used a conservative cathode thermal emittance estimate of 1 μm/ mm rms [5] and we present results from the LCLS-II injector to show the emittance improvements we could expect if we were able to improve the thermal emittance. Accordingly, we froze the positions of the components of the beamline to correspond to the injector that is currently being built at SLAC. The knobs we varied and the layout of the LCLS-II injector are shown in Table 1 and Fig. 2. The Pareto Fronts achieved are displayed in Fig. 3.

ANALYSIS

LCLS-II is interested in a beam with a longitudinal bunch length around 1 mm at the end of the injector so we manually picked the lowest emittance population member in the 0.9-1.2 mm range to compare here (see Table 2). All displayed results are with 10,000 ASTRA particles with 100 pC. However, there is typically a 10% emittance reduction when 200,000 ASTRA particles are used with finer meshing. We plot the energy spread, 95% rms transverse emittance and the bunch length as a function of the injector position, Z, to show which variables had to change to accommodate either a harder constraint value, or more spot size dependent emittance off of the cathode.

Reaching the 200 keV energy spread specification was immediate. Achieving the 5 keV HO energy spread constraint was more difficult. No configuration initially met the HO constraint and the only populations that could survive had a smaller cathode spot size and shorter initial bunch lengths. The HO energy spread was then mostly fixed by adjusting the cavity 4 phase as visually show in the energy spread plot in Fig. 4. Because the HO energy spread constraint already necessitated the smaller spot size, the knobs did not change very much when the cathode

ISBN: 978-3-95450-217-2 doi:10.18429/JACoW-ERL2019-WEPNEC21

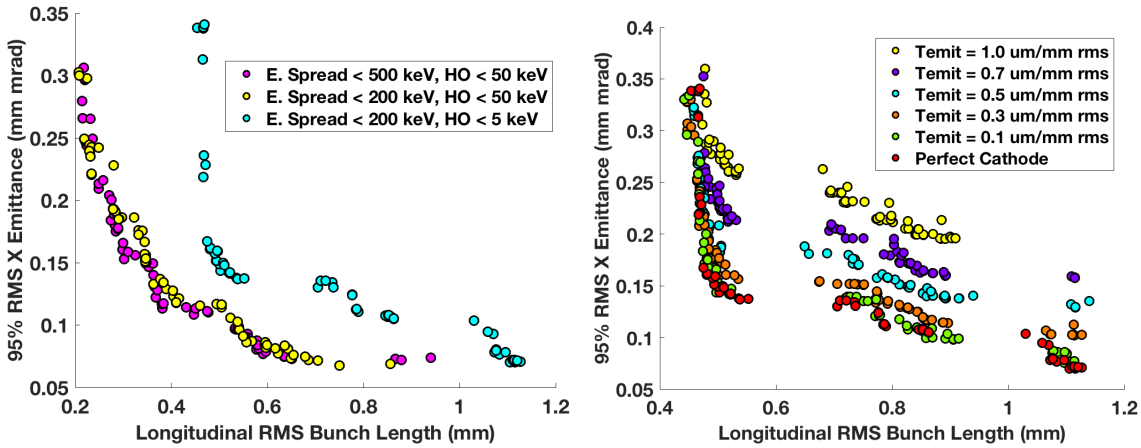

Figure 3: Pareto Fronts that show the impact of FEL specific energy constraints with a zero emittance cathode (left) and the dependence of the cathode emittance on the final emittance (right)

Table 2: Upgrade Emittance Table. All configurations were evaluated with 10,000 ASTRA particles

APEX Configuration	Emit. at Cathode mm mrad	100 % X Emit mm mrad	95 % X Emit mm mrad	Long. Size mm	E.Spread keV
E. Spread $<$ 500 keV, HO $<$ 50 keV	0	0.111	0.074	0.94	296.7
E. Spread $<$ 200 keV, HO $<$ 50 keV	0	0.108	0.069	0.86	157.7
E. Spread $<$ 200 keV, HO $<$ 5 keV	0	0.113	0.070	1.11	66.6
Thermal Emit = 0.1 $\frac{\text{mm mrad}}{\text{mm rms}}$	0.017	0.122	0.076	1.1	104
Thermal Emit. = 0.3	0.054	0.152	0.103	1.07	131.9
Thermal Emit. = 0.5	0.087	0.181	0.130	1.12	77.2
Thermal Emit. = 0.7	0.122	0.215	0.158	1.12	76.9
Thermal Emit. = 1.0	0.16	0.261	0.196	0.91	185.4

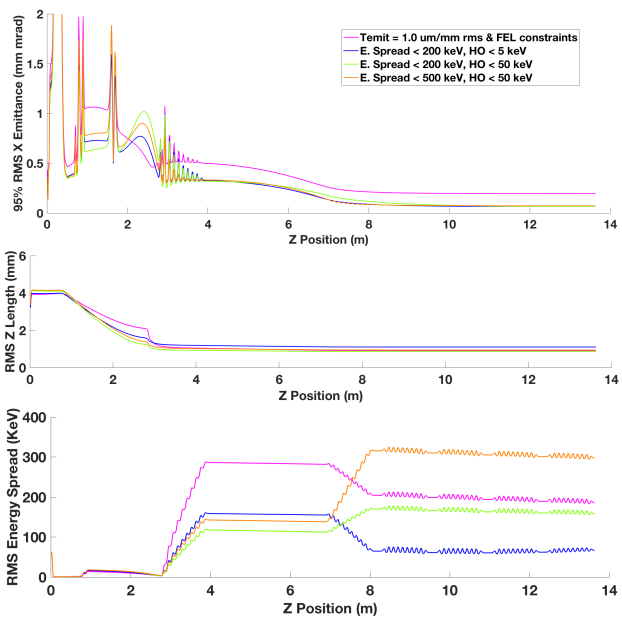

Figure 4: Emittance, bunch length and energy spread comparisons for a population with an end bunch length around 1 mm. The blue, orange, and green plots are all with a zero emittance cathode.

emittance was added back in.

CONCLUSION

We seek to understand the individual cathode and lattice emittance contributions towards the final injector emittance. The Pareto Fronts start documenting the benefits from further cathode research for the LCLS-II injector system. Keeping in mind that the 95% rms transverse emittance reliably decreases around 10% when 200,000 ASTRA particles are used, the results with the current LCLS-II injector indicate we would need a cathode around 0.3 μm/ mm rms to feasibly achieve 0.1 mm mrad 95% emittance at the end of the injector.

The main limitation of this study is that there is no way to definitively know that the Pareto Fronts are truly the global optimum. We played with the mutation and crossover parameters, but a perfect recipe of number of generations, algorithm parameters and ASTRA particle size that prevents getting in local minimum with reasonable computation time is still elusive.

REFERENCES

[1] T. Raubenheimer, "LCLS-II-HE FEL Facility Overview". Workshop on Scientific Opportunities for Ultrafast Hard X-rays at High Rep. Rate. Sept. 2016, SLAC.

ISBN: 978-3-95450-217-2 doi:10.18429/JACoW-ERL2019-WEPNEC21

https://portal.slac.stanford.edu/sites/conf_public/lclsiihe2016/Pages/default.aspx

[2] Z. Huang, K.J. Kim. "Review of x-Ray Free-Electron Laser Theory" *Phys. Rev. ST Accel. Beams*, vol. 10 (3), p. 034801, 2007. doi:10.1103/PhysRevSTAB.10.034801

[3] F. Zhou *et al.*, "LCLS-II Injector Physics Design and Beam Tuning", in *Proc. IPAC'17*, Copenhagen, Denmark, May 2017, pp. 1655–1658. doi:10.18429/JACoW-IPAC2017-TUPAB138

[4] C. F. Papadopoulos *et al.*, "RF Injector Beam Dynamics Optimization for LCLS-II", in *Proc. IPAC'14*, Dresden, Germany, Jun. 2014, pp. 1974–1976. doi:10.18429/JACoW-IPAC2014-WEPRO015

[5] C. Mitchell *et al.*, "Beam Dynamics Optimization in High-Brightness Electron Injectors", presented at FEL'17, Santa Fe, NM, USA, Aug. 2017. paper: THB01, unpublished.

[6] K. Floettmann, "ASTRA: A Space Charge Tracking Algorithm", user's manual available at http://www.desy.de/~mpyflo/

[7] D. Kalyanmoy *et al.*, "Fast and Elitist Multiobjective Genetic Algorithm: NSGA-II". IEEE Transaction on Evolutionary Computation, vol. 6, no. 2, Apr. 2002, pp. 182-197. doi:10.1109/4235.996017

[8] K. Floettmann, "Some Basic Features of the Beam Emittance", *Phys. Rev. ST Accel. Beams*, 6, p. 034202 (2003). doi:10.1103/PhysRevSTAB.6.034202

[9] T. Rao, and D. Dowell. "An Engineering Guide to Photoinjectors". CreateSpace Independent Publishing, 2013. arXiv:1403.7539[physics.acc-ph]

[10] F. Sannibale *et al.*, "Status of the APEX Project at LBNL", in *Proc. IPAC'14*, Dresden, Germany, Jun. 2014, pp. 727–729. doi:10.18429/JACoW-IPAC2014-MOPRI054